Remote Sensing of the Coastal Ocean with Standard Geodetic GNSS-Equipment

Johan S. Löfgren[1], Rüdiger Haas[1], Kristine M. Larson[2], Hans-Georg Scherneck[1]

johan.lofgren@chalmers.se, rudiger.haas@chalmers.se, kristinem.larson@gmail.com, hans-georg.scherneck@chalmers.se

[1]Chalmers University of Technology, Department of Earth and Space Sciences, Onsala Space Observatory, SE-439 42 Onsala, Sweden

[2]University of Colorado, Department of Aerospace Engineering Sciences, UCB 429, Boulder, CO 80309-0429, USA

CARRIER PHASE METHOD

GNSS carrier phase data from both the direct signal (RHCP) and the reflected signal (LHCP) are analyzed.

The reflected signals experience an additional path delay compared to the direct signals, see ***Figure 2***.

– *The LHCP antenna can be regarded as a virtual antenna located below the sea surface.*

When the sea level changes, the path delay of the reflected signal changes, thus the LHCP antenna will appear to change position.

Since the height of the LHCP antenna over the sea surface is directly proportional to the sea surface height and the RHCP antenna is directly proportional to the land surface height, the installation monitors:

– *sea surface height,*
– *land surface motion,*
– *sea level independent of land motion.*

Figure 3 *– The GNSS-based tide gauge facing south.*

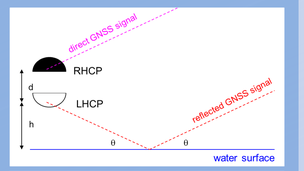

Figure 2 *– Schematics of the carrier phase method; receiving both direct and reflected satellite signals.*

The dataset consists of 8 months of 1 Hz sampled GNSS data from SEP 16, 2010 to MAY 31, 2011:

– *the reflected signals have a lower SNR than the direct signals,*
– *there are less observations from the LHCP antenna than from the RHCP antenna (open sea surface only to the south, see **Figure 3**),*
– *it is a kinematic situation due to a moving sea surface.*

Processing with an in-house single difference software in MATLAB, with the solution setup:

– *Global Positioning System (GPS) L_1 carrier phase observations,*
– *broadcast satellite ephemerides,*
– *application of elevation and azimuth mask,*
– *20 minutes of data,*
– *horizontal baseline fixed.*

Least-squares solution with estimation of:

– *vertical baseline **Δv** between the antennas (for each 20 minute interval),*
– *phase ambiguity differences (for each satellite)*
– *receiver clock bias differences (each epoch).*

Vertical baseline is converted to local sea level by: ***Δv=2h+d***, *see **Figure 2***.

METHOD COMPARISON

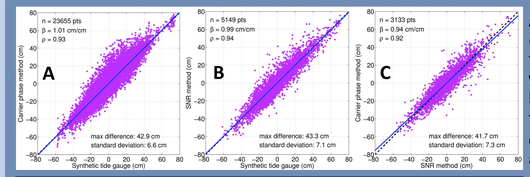

Figure 8 *– Scatter plots of the sea level for the phase and the SNR method versus sea level from a synthetic tide gauge, **A** and **B**, respectively, and for the phase method versus the SNR method, **C**. Number of points (n), rate coefficient (β), correlation coefficient (ρ), max difference, and standard deviation are presented in each subfigure.*

A Synthetic Tide Gauge (STG) record was created from records of two stilling well gauges 18 km and 33 km away from OSO.

Time series of the datasets (CP, SNR, STG) are presented in ***Figure 7***.

Figure 8 depicts pairwise scatter plots.

Results of an ocean tidal analysis are presented in ***Figure 9***.

INTRODUCTION: THE GNSS-BASED TIDE GAUGE

The Global Navigation Satellite System (GNSS)-based tide gauge is installed at the Onsala Space Observatory (OSO), measuring sea level using GNSS signals reflected off the local sea surface, see *Figure 1*. The installation consists of two antennas, one zenith-looking Right Hand Circularly Polarized (RHCP) and one nadir-looking Left Hand Circularly Polarized (LHCP). Each antenna is connected to a standard geodetic GNSS receiver. Sea level is estimated using two different methods:

I. ***CARRIER PHASE METHOD:*** Carrier Phase (CP) from both receivers (the direct signals from the RHCP antenna and the signals reflected off the sea surface from the LHCP antenna) are used in standard geodetic processing.

II. ***SIGNAL-TO-NOISE RATIO METHOD:*** Signal-to-Noise Ratio (SNR) values from only the receiver connected to the RHCP antenna are analyzed (the SNR is affected by the signals reflected off the sea surface reaching the antenna backside, a.k.a. multipath).

Figure 1 *– The GNSS-based tide gauge at OSO.*

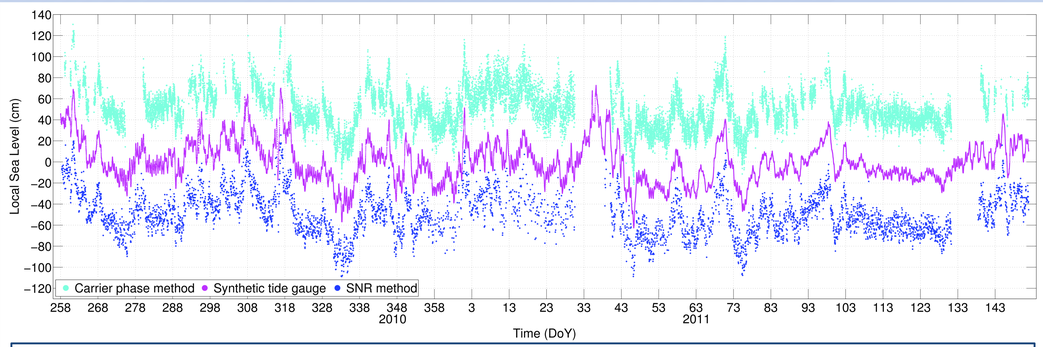

Figure 7 *– Local sea level in cm from the GNSS-based tide gauge at OSO from carrier phase and signal-to-noise ratio analysis, top **cyan** and bottom **blue**, respectively, and from a synthetic tide gauge at OSO, constructed from stilling well gauge observations at Gothenburg and Ringhals (approximately 33 km north and 18 km south of OSO, respectively), centre **magenta**. To improve visibility, the GNSS-derived sea level time series are presented with an offset of plus and minus 50 cm. The times series cover September 16 (DoY 258), 2010 to May 31 (DoY 151), 2011.*

CONCLUSIONS

The GNSS-derived sea level, using the carrier phase and the SNR method, resembles well the synthetic tide gauge sea level:

– *the standard deviations are 6.6 cm (CP-STG), 7.1 cm (SNR-STG), and 7.3 cm (CP-SNR),*
– *the correlation coefficients are larger than 0.92.*

From ocean tide analysis, several major tidal components are determined significantly and show agreement with results derived from the stilling well gauge data.

We are convinced that the GNSS-based tide gauge has large potential for oceanography due to:

– *remote sensing, i.e., no need for immersed instrumentation,*
– *standard geodetic GNSS-equipment and analysis,*
– *continuous measurements with high temporal resolution and good agreement to traditional tide gauges,*
– *a new dataset for tidal analysis and improvement of tidal models,*
– *applicable at the coast, on off-shore platforms, and even in tectonically active regions.*

SIGNAL-TO-NOISE RATIO METHOD

GNSS SNR data from the direct signal (receiver connected to the RHCP) are analyzed.

The satellite signals reflected off the sea surface interfere with the direct signals, known as multipath, see ***Figure 4***. This causes oscillations in the SNR data, see ***Figure 5A***.

From the SNR oscillations it is possible to determine the vertical distance between the antenna phase centre and the reflecting sea surface.

– *This distance is directly proportional to the sea surface height.*

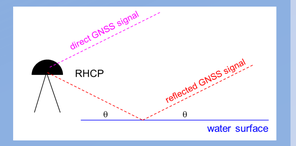

Figure 4 *– Schematics of the SNR method: receiving the direct signal and the reflected signal as multipath.*

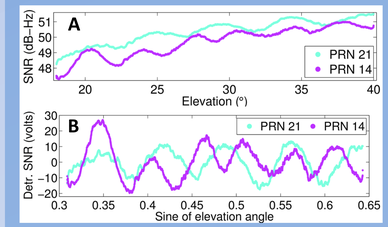

Figure 5 *– Original (**A**) and detrended SNR data (**B**) for two satellite arcs of day-of-year 316 (2010). The observations from satellites with Pseudo Random Noise (PRN) number 21 (**cyan**) and 14 (**magenta**) correspond to low (morning) and high sea level (night), respectively.*

The dataset consists of 8 months of 1 Hz sampled GPS L_1 SNR data from SEP 16, 2010 to MAY 31, 2011.

For each satellite arc (rising or setting) the original SNR data, ***Figure 5A***, were converted to natural units and detrended by fitting and removing 2:nd order polynomials.

Assuming that the sea level does not change for a satellite arc, the oscillation frequency of the detrended SNR data is constant as a function of sine of the satellite elevation angle, see ***Figure 5B***.

In order to estimate local sea level height from the SNR data, the Lomb Scargle Periodogram (LSP) method was used.

The peak frequency of each LSP (see ***Figure 6***) was converted to reflector height (by scaling with ½ times the carrier wavelength).

A large reflector height value corresponds to a low sea level and vice versa.

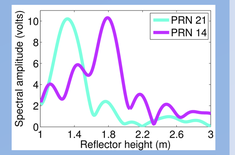

Figure 6 *– LSP for the SNR data presented in Figure 5.*

OCEAN TIDE ANALYSIS

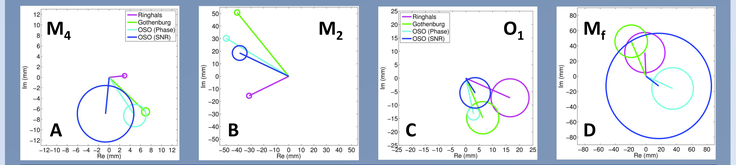

Figure 9 *– An ocean tide analysis of the GNSS-derived sea level (carrier phase, **cyan**, and SNR, **blue**, method) determined several major tidal components significantly, e.g., M_4 (**A**), M_2 (**B**), O_1 (**C**), and M_f (**D**). As a comparison, the analysis was also made for the stilling well gauges at Ringhals, **magenta**, and Gothenburg, **green**, 18 km south and 33 km north of OSO, respectively.*